HOW TO REDUCE THE HARD ROCK MINING INDUSTRY'S COMMINUTION CARBON FOOTPRINT BY UP TO 40%

Stephen Morrell
Managing Director
SMC Testing Pty Ltd

ABSTRACT

Comminution is a major contributor to the Mining Industry's carbon footprint. As most of the world's leading mining companies have formally committed themselves to having net zero scope 3 carbon emissions by at the latest 2050, the pressure to significantly improve comminution circuit energy efficiency over the next 25-30 years will be intense.

A detailed study of the current carbon footprint from comminution in hard rock mining has shown that annual CO_2 emissions are of the order of 75 Megatonnes. A very large proportion of this is generated by Semi-autogenous (SAG)/Ball mill circuits through a combination of electricity consumption and so-called embedded energy in the manufacture of steel grinding balls. High Pressure Grinding Rolls (HPGR) circuits have the potential to reduce these emissions by up to 32.8 Megatonnes/year, or 44.3% when compared to the Semi-autogenous/ball mill circuit alternatives. However, uptake of HPGR technology has been relatively slow despite the fact that it is considered to be a reasonably mature technology. This may be due in part to the fact that costly and time-consuming pilot testing is still the norm for assessing, selecting and sizing HPGR circuits. This is in contrast to SAG/Ball mill circuits where relatively cheap, fast and effective power-based methodologies are used.

To combat this limitation and help accelerate the adoption of this technology a power-based methodology has been developed which can be easily used to assess, size and select HPGR closed circuits in hard rock mining applications. Equations are derived which, on the basis of published data from manufacturers and full-scale operating plants, are demonstrated to accurately reproduce HPGR throughput capacity, installed power and specific energy for a wide range of HPGRs

1 INTRODUCTION

All industries are facing increasing pressure to ensure that carbon emissions are reduced to help achieve the so-called 1.5° C future. This has led to most of the major mining companies committing to significant reductions in their operational carbon footprint – in many cases by up to 30-40% in the next 10-15 years - and to place themselves in a net-zero scope 3 emissions position by 2050. Comminution has been identified as a relatively large consumer of electrical energy, reportedly being responsible in some cases for over 50% of a mine-sites power requirement (Daniel et al, 2010; Buckingham et al, 2011) and consequently is responsible for a significant proportion of many mining company's carbon footprints. Currently Autogenous (AG)/Semi-Autogenous (SAG)/Ball mill technology dominates comminution circuit design where grinding to relatively fine sizes is required, eg. the gold, copper, nickel, platinum, silver, lead, zinc and low grade iron ore sectors. High Pressure Grinding Rolls (HPGR) have been found to be more energy efficient than tumbling mills such as AG/SAG and ball mills and, having been invented by the late Prof. Schönert 45 years ago, is now considered to be a relatively mature technology. However, despite its proven savings in energy and carbon emission, uptake in the technology has been relatively slow. This in part may be due to the fact that pilot testing, with all of its attendant high costs and lengthy execution time, is still seen as the principal method of obtaining data from which HPGR trade-off studies and subsequent bankable feasibility studies are based. Having a proven power-based route to cheaply, quickly and accurately assess, size and select HPGR circuits might alleviate this limitation and help accelerate adoption of this energy/carbon-saving technology.

In this paper a power-based methodology for sizing HGPR circuits closed with classifiers is described in detail and uses recently published data from a number of operational full-scale circuits to prove its validity. Much of the paper targets hard rock applications for HPGR-Ball mill circuits but the more energy efficient HPGR-HPGR alternative is also included.

2 HISTORIC PERSPECTIVE OF AG/SAG AND HPGR CIRCUITS

2.1 AG/SAG Mill Circuits

30 years ago AG/SAG mill circuits were still almost exclusively sized using data from pilot test programs. These were both expensive and time consuming to conduct and necessitated the use of hundreds of tonnes of sample material. This material was normally sourced via trenches that were blasted and excavated from the surface of the deposit. Not only was this also expensive it left the question unanswered as to whether the sample was representative of the entire deposit. In many cases ore deposits become harder as depth increases and caused the problem that AG/SAG circuits designed on the basis of (softer) surface samples ran the risk that after a few years when the ore became harder they would be unable to maintain target throughput. Nowadays it is rare that such pilot testing is used. Instead relatively cheap and accurate power-based techniques are used following the development of equations which accurately predict the specific energy and power draw of AG/SAG and ball mills (Morrell, 1996, 2004[a],2004[b]; Sinto et al., 2015, Lane et al., 2013), combined with the development of laboratory ore characterisation tests that could be carried out on small diameter drill core and that accurately reflected changes in hardness with respect to AG/SAG mill performance and location within the deposit. The development of accurate comminution simulation models and user-friendly computer programs such as JKSimMet further assisted in obviating the need for pilot test programs for AG/SAG mill circuits and helped fuel the adoption of AG/SAG technology to the point where it now dominates comminution circuit design in the Mining Industry.

2.2 HPGR Circuits

The HPGR was invented by the late Prof. Schönert, who was granted a patent in 1977 (Rashidi et al, 2017). By 1984 the technology was being used in the cement industry and by the late 1980's was followed by the diamond and iron ore industries (Klymowski, 2003; CIM Magazine, 2018). In the case of the diamond industry, HPGRs were chosen for their enhanced liberation action whilst in iron ore processing HPGRs were used in iron ore pellet feed applications to enhance surface specific area (van der Meer, 1997, 2015) as well as for tertiary/pebble crushing (van der Meer and Maphosa, 2012; Mcivor et al, 2001). In neither application was the HPGR principally chosen for its energy efficiency and almost a further 20 years had to pass before the Mining Industry saw the first full scale HPGR-Ball mill installation at Cerro Verde (Vanderbeek et al, 2006), which was chosen due to the 15% energy saving it provided compared to the SAG-Ball mill alternative. Several HPGR-Ball mill circuits have subsequently been successfully designed and installed, mainly in the copper/gold sectors such as Boddington (Hart et al, 2012), Tropicana (Kock et al, 2015), Salobo (Burns et al, 2019), Morenci (Mular et al, 2015) and Sierra Gorda (Comi and Burchardt, 2015). In all cases design of the circuit and equipment selection was based on extensive pilot testing. More recently a HPGR-HPGR dry-processing circuit has been chosen for the Iron Bridge Magnetite Project instead of the AG-ball mill alternative (Fortescue, 2019). Following an extensive on-site pilot program costing $500 million, Fortescue reported that the results indicated energy savings of over 30% (Mining Technology, 2021). However, despite these successes uptake of this technology in the Mining Industry remains slow.

3 ESTIMATING COMMINUTION'S ELECTRICITY CONSUMPTION

3.1 Using AG/SAG/Ball Mill Circuit Installed Motor Capacity

Tozlu and Fresko (2015) estimated that the total installed motor capacity of AG/SAG mills in hard rock mining in 2015 was 5.8 million kW (see Figure 1), being dominated by copper, gold, iron, zinc/lead, nickel and platinum ores, ie by the hard rock mining industry. Given that mining industry activity has been relatively slow since then, additional sales of AG/SAG mill capacity from then until now would possibly be no more than 0.5 million kW. If a service life of 50 years for AG/SAG mills is assumed, then all pre-1971 sales (about 0.3 million kW) are likely to be out of use by now. Based on these assumptions it is therefore estimated that the current installed motor capacity of AG/SAG mills is about 6 million kW. Although there are a number of single stage AG/SAG mill circuits, in the vast majority of cases comminution circuits comprise AG/SAG mills followed by ball mills.

Tozlu and Fresko's data indicate that the global installed motor capacity of AG/SAG-Ball mill circuits is split approximately 42:58 between the AG/SAG mill and ball mill circuits respectively. Thus, assuming that the global 2021 AG/SAG motor capacity is 6.0 million kW, the estimated combined AG/SAG/Ball mill installed motor capacity is of the order of 14.3 million kW. Assuming 90% utilisation of the installed power, annual operating hours of 8000 (91.3% availability), and a 3% allowance for motor losses, equates to an estimated annual electricity consumption by AG/SAG/Ball mills of 106 TWh (106 billion kWh). Note that this represents only electricity consumed in the mills, ie it does not include ancillaries. 44.5 TWh is estimated to have been consumed in the AG/SAG mill circuits and 61.5 TWh in the ball mill circuits.

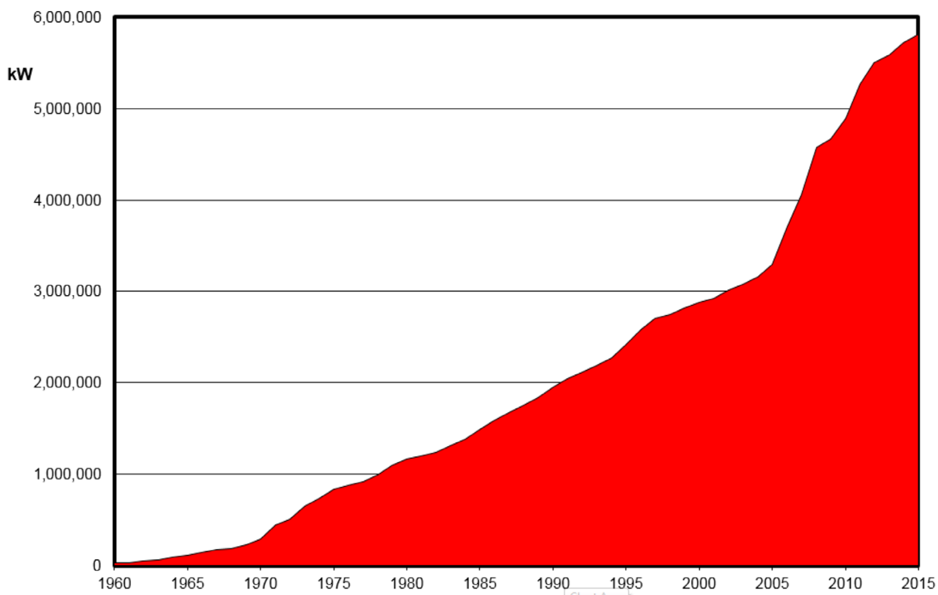

Figure 1 – Cumulative Installed Power of AG/SAG Mills (after Tozlu and Fresko, 2015)

3.2 Using Tonnes Milled and Specific Energy Estimates

An alternative way of estimating comminution machine electrical energy consumption in the hard rock mining sector is, for each commodity covered by this sector, to multiply the total ROM ore tonnes processed by the overall specific energy of the comminution circuit. These results can then be summed across all sectors to arrive at an estimated total electrical energy consumption. To arrive at estimates of how many tonnes of ore in each of the commodities is comminuted it is first necessary to find out what the global production of each commodity is. These data are usually reported by global institutes/associations/government bodies dedicated to providing such information. Using estimates of typical ore grades and recoveries, the total tonnes of ore of each commodity that is comminuted can be estimated from:

$$Tonnes\ comminuted = Tonnes\ of\ commodity \div grade \div recovery \qquad (1)$$

The next step is to estimate the total specific comminution energy for each ore. To do this, use was made of Morrell's energy-size relationship. The general form of this equation is:

$$W = M_i \times 4 \times \left({P_{80}}^{f(P80)} - {F_{80}}^{f(F80)}\right) \qquad (2)$$

Where:

W = predicted circuit net specific energy
M_i = hardness parameter
$f(x)$ = $-(0.295 + x/1000000)$
x = 80% passing size in microns

A full description of this equation and worked examples of how it is used can be found in a number of published sources ((Morrell, 2004[b]; GMG Group, 2021, Morrell, 2022) and on-line (https://www.smctesting.com/tools/comminution-specific-energy).

For AG/SAG/Ball mill circuits the hardness parameters Mia® and Mib® are required. The Mia® value comes from the SMC Test® and use of the SMC Test® data base of over 65000 values was made to extract the mean Mia® value for each ore type. The Mib® is determined from the output of a standard Bond ball work index test. Data from the author's studies of over 100 comminution circuits plus published sources (principally SAG conference volumes over the period 1989-2015) were used to obtain typical mean Bond ball work index values from which Mib® values were estimated.

The resulting energy estimates are shown in Table 1. The total estimated electricity consumption for comminution was 132.9 TWh. Comparing the AG/SAG/Ball mill estimate in the previous section of 106 TWh suggests that possibly the difference (20%) is due to consumption of electricity in other comminution circuit designs such as crushing/ball, rod/ball, HPGR/ball, ball/ball and crushing only (eg DSO iron ore). Whereas it is likely that this is a major contributing factor, inaccuracies in the data and assumptions made in each methodology might also be a contributing factor.

What is interesting from both analyses in that, based on the global electricity consumption reported by the International Energy Authority, comminution in hard rock mining amounts to, at most, 0.6%. Interestingly this is a similar figure to that produced by the landmark study in 1981 by the NRC (National Research Council,1981) which reported that for the same commodities included in Table 1 the associated figure for the USA was 0.45%. These figures seem at odds with most of the published quotes on comminution's contribution to global electricity demand which put the figure far higher, eg the CEEC puts it at up to 5 times higher (https://www.ceecthefuture.org/). Be that as it may, even at 0.6% of the world's electricity consumption the associated greenhouse gas emissions are considerable and will need to be reduced in the next decade. For the purposes of this paper, which concentrates on the impact of using HPGR technology to replace AG/SAG/Ball mill circuits, a figure of 106 TWh will be used.

Table 1 - Estimated Electricity Consumption By Comminution Per Commodity In The Hard Rock Mining Industry

commodity	electricity consumption	
	TWh	%
copper	52.4	39.4
iron - low grade	35.6	26.8
gold	15.9	12.0
zinc & lead	8.6	6.4
nickel	8.0	6.0
phosphate	4.4	3.3
silver	1.8	1.4
alumina	1.7	1.2
iron - high grade (DSO)	1.7	1.3
platinum	1.3	1.0
uranium	0.5	0.3
other	0.9	1.1
total	132.9	100
total global electricity*	22,848	100
total hard rock mining	132.9	0.6

*based on 2019 data

4 ESTIMATING COMMINUTION'S CARBON FOOTPRINT

4.1 Electricity Consumption

The data in the previous sections relate to the direct consumption of electricity, eg as it is read from a kWh meter. The generation of this electricity results in emissions of $C0_2$ and other gases harmful to the environment. The extent to which this happens varies from location to location and depends on how the electricity is being generated. Coal-fired electricity generation for example produces the largest amount of carbon emissions, whilst nuclear, wind and solar produce the least. Globally the proportion of electricity generated by different methods is changing all the time, the current push being to reduce fossil-fuel use in favour of renewable sources such as wind and solar. For the purposes of calculations in this paper, the 2020 distribution of electricity generation by source has been taken from World Energy Data (2021) (see Figure 2). Direct CO_2 emissions per kWh of electricity generated by each of these sources have been taken from the Energy Information Administration of the USA government (EIA, 2020), whilst data on lifecycle CO_2 emission of different electricity generating sources have been taken from Pehl et al (2017). Combining these data produces an estimated global emissions rate of 0.556 kgs CO_2/kWh of electricity generated. This equates to 0.556

megatonnes/TWh. Using 106 TWh as the AG/SAG/Ball mill annual consumption of electricity in the hard rock mining sector gives an estimated 58.9 megatonnes of CO_2 emissions.

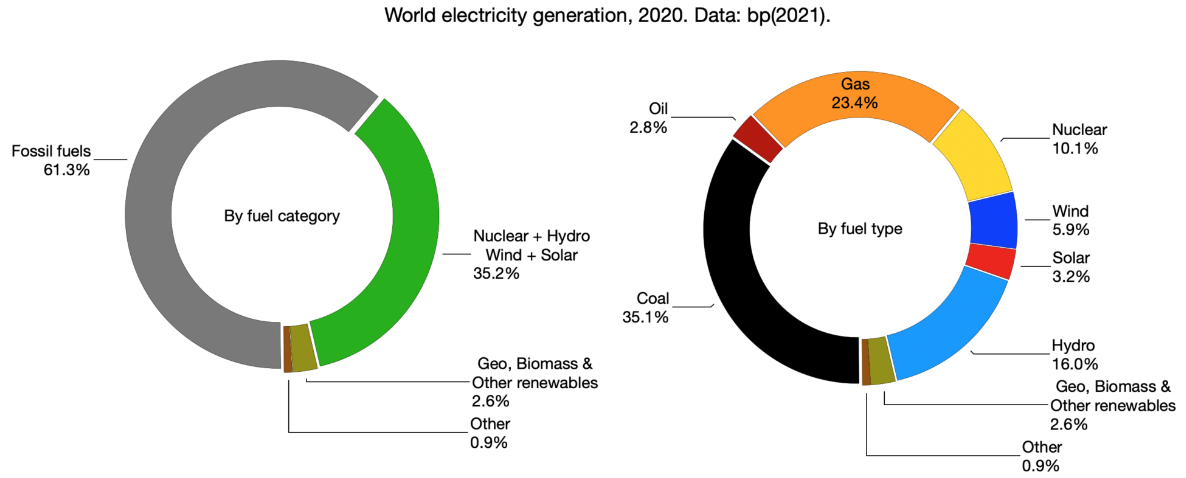

Figure 2 – Global Electricity Generation by Source for 2020 (after World Energy Data, 2021)

4.2 Steel Wear

Whereas it is the direct electricity consumption of comminution circuits that normally has the most attention focused on it, there are also indirect or so-called "embedded" energies that also need to be taken into consideration as they have associated CO_2 emissions. The principal source of these embedded carbon emissions is from the manufacture of steel balls which have to be regularly added to SAG and ball mills as the balls wear away (Daniel, 2007). Ball wear rates are normally represented in terms of kgs (or grams) of steel per kWh of electrical energy directly consumed by the mill. Giblett and Seidel (2011) provide steel ball wear rates from twelve of Newmont's grinding circuits from around the world and which on average give ball wear rates of 0.081 kgs/kWh and 0.049 kgs/kWh for their SAG and ball mills respectively. Assuming these figures are reasonably representative of all SAG-Ball mill circuits, then, If they are multiplied by the annual electricity consumption of SAG and ball mills the global annual consumption of steel balls can be estimated. Of course steel balls are not used in AG mills. Such mills are relatively rare and are estimated to account for no more than 3% of global motor capacity. Hence, making allowance for AG mills and omitting energy for ancillaries gives estimated direct annual electricity consumptions by SAG mills and ball mills of 43.2 TWh and 61.5 TWh respectively. On this basis the estimated annual steel ball consumptions of SAG mills and ball mills is 3.48 million tonnes and 3.06 million tonnes respectively – a total of 6.54 million tonnes/year. The World Steel Association (2017) gives a figure of 1.9 kgs of CO_2 emitted per kg of crude steel produced. Subsequent forging/casting to obtain the finished product adds, on average, a further 0.41kgs of CO_2 (Demus et al,2012; Dindorf and Wos, 2020) giving a total of 2.31 kgs CO_2 emitted per kg of steel balls consumed. This equates to a total of 15.1 megatonnes of additional CO_2 emissions per year for AG/SAG-Ball mill circuits.

4.3 Total Comminution

"Total" in this case is defined as the sum of greenhouse gas emissions by AG/SAG/Ball mill machines' use of electricity and steel balls consumption by SAG/Ball mills and does not include the contribution of ancillaries. Table 2 summarised the estimated total CO_2 emissions from each source and its contribution to global emissions. It can be seen that in total it is estimated that AG/SAG/Ball mills were responsible for 74.0 Megatonnes of CO_2 emissions, which represents 0.22% of global emissions.

Table 2 - Estimate of the Total Annual Contribution of CO_2 Emissions by AG/SAG/Ball Mills in the Hard Rock Mining Sector*

source	Megatonnes CO_2	%
electricity consumption	58.9	0.178
steel ball consumption	15.1	0.046
total	74.0	0.224

global	33000	100

*based on 2019 data

5 POTENTIAL FOR GLOBAL CARBON EMISSION SAVINGS USING HPGR TECHNOLOGY

Although it is perhaps unrealistic to expect that all of the existing AG/SAG-Ball mill circuits would be replaced by HPGR circuits in the near future, there have been a number of cases where HPGR's have been integrated into existing circuits with significant efficiency improvements, such as Empire, (Dowling et al, 2001), Penasquito (Palmer et al, 2011), Freeport (Villanueva et al, 2011), Cadia Hill (Engelhardt et al, 2015) and Mogalakwena (Rule et al, 2015). It is therefore worthwhile estimating what the maximum potential global impact on carbon emissions could be if HPGRs were to replace or at least be integrated with existing AG/SAG/Ball mill circuits.

5.1 HPGR-Ball Mill Circuits

If only the energy consumption of the comminution machines is considered when comparing AG/SAG-Ball mill with HPGR-Ball mill circuits then typically the latter circuits are reported to use of the order of 20-25% less energy. However, ancillaries (conveyors, screens, transfer pumps, cyclone slurry pumps, dust extraction etc) in the HPGR-Ball mill circuit are more energy intensive and when they are taken into account the energy savings are of the order of 15% overall (Parker et al, 2001, Koski et al, 2011, Kock et al, 2015). Using an overall electrical energy saving of 15% for the HPGR-Ball mill circuit compared to the AG/SAG-Ball Mill circuit equates to a potential global saving in CO_2 emissions of 8.8 megatonnes/year.

As HPGR-Ball mill circuits do not have the burden of embedded CO_2 emissions from SAG mill steel ball consumption, only the ball mill circuit needs to be considered. Ball mills in HPGR-Ball mill circuits tend to have more installed capacity than their counterparts in AG/SAG-Ball mill circuits. This is because the product size distribution from AG/SAG mills tends to have more fine material than the HPGR circuit product (Morrell, 2009; 2011) and hence need less ball mill power. Based on data from Koski et al (2011) and Kock et al (2015) a ball mill in a HPGR-Ball mill circuit will need about 20% more power than one in a SAG-ball mill circuit. On this basis it is estimated that the steel ball consumption of ball mills in HPGR circuits would be 3.67 million tonnes per year – a saving of 2.87 million tonnes per year compared to SAG–Ball mill circuits. This equates to a reduction in emissions of 6.6 megatonnes of CO_2 per year. Combined with the emissions saving due to the HPGR's better energy efficiency gives a total saving of 15.5 megatonnes of CO_2 / year or 20.9% compared to AG/SAG-Ball mills (see Table 3).

Table 3 – Estimated Annual CO_2 Emissions Saving for HPGR-Ball Mill Circuits in the Hard Rock Mining Sector (Figures in megatonnes of CO_2 per year)

source	AG/SAG/Ball	HPGR/Ball	HPGR Circuit Savings	
			absolute	%
electricity consumption	58.9	50.1	8.8	15.0
steel ball consumption	15.1	8.5	6.6	43.9
total	74.0	58.5	15.5	20.9

5.2 HPGR-HPGR Circuits

AG/SAG mills have similar energy efficiencies to ball mills (Morrell, 2004b). Hence, if by replacing AG/SAG mills with HPGRs energy savings of 15% are realised, then if ball mills are also replaced similar additional energy savings could be expected. This is what Fortescue Minerals found in their large scale pilot/demonstration plant at Iron Bridge (Fortescue, 2019) which is illustrated in Figure 3. The first stage of HPGR size reduction has a similar duty to that used in HPGR-Ball mill circuits, whilst the second stage HPGR circuit replaces the relatively fine grinding that the ball mills provide. The use of HPGRs for relatively fine grinding is not new, being found in similar duties in the cement industry (Aydoğan at al, 2006) and for grinding iron ore pellet feed (van der Meer, 2015).

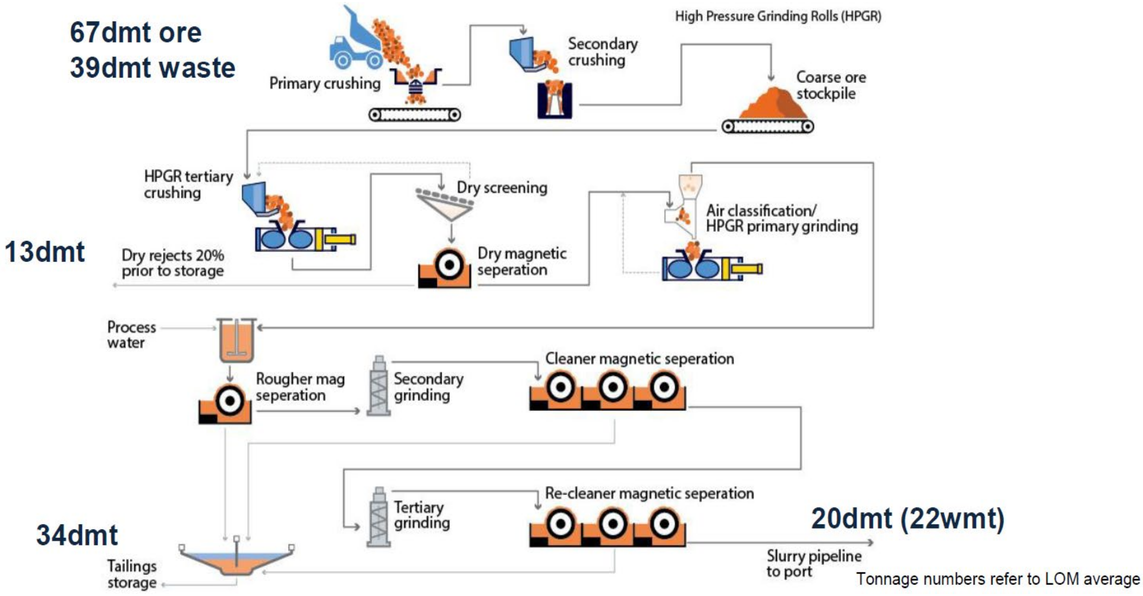

Figure 3 – Process Flowsheet for Iron Bridge Magnetite (Fortescue, 2019)

If the same calculation route for estimating potential global energy and CO_2 savings in section 5.1 is applied to the HPGR-HPGR circuit the results shown in Table 2 are obtained. In this case it was assumed that overall energy savings amounted to 30%, as per the Iron Bridge experience. Hence potential emissions savings from improved energy efficiency amount to an estimated 17.7 megatonnes per year.

As there are no SAG mills and no ball mills in the HPGR-HPGR circuit there are additional savings in CO_2 from the fact that steel ball consumption is zero. A further 15.1 megatonnes of CO_2 is therefore estimated to be potentially saved, giving a total saving of 32.8 megatonnes of CO_2 or 44.3% compared to a AG/SAG-Ball mill circuits.

This is a huge potential saving whose realisation might be speeded up if a relatively simple, cheap yet accurate methodology were available to assess, select and size HPGR-Ball mill and HPGR-HPGR circuits, instead of the very costly and time-consuming piloting route that is currently adopted. Such a methodology, incorporating power-based techniques, will be described in detail in the following sections.

Table 4 – Estimated Annual CO_2 Emissions Saving for HPGR-HPGR Circuits in the Hard Rock Mining Sector (Figures in megatonnes of CO_2 per year)

source	AG/SAG/Ball	HPGR/HPGR	HPGR Circuit Savings	
			absolute	%
electricity consumption	58.9	41.2	17.7	30.0
steel ball consumption	15.1	0.0	15.1	100.0
total	74.0	41.2	32.8	44.3

6 POWER-BASED METHODOLGY FOR SIZING HPGR CIRCUITS

6.1 General

The so-called power-based methodology is the current mainstay of processing engineers for helping to size and select conventional crushers, AG/SAG mills and ball mills. The methodology involves a number of steps, most of which are broadly similar regardless of the comminution circuit. However, the details in each step may differ slightly depending on the type of equipment being considered. These steps are as follows:

i. Using breakage (hardness) parameters from laboratory tests on representative ore samples, the net specific energy (kWh/t) of the machine in question is estimated. In the case of closed circuits whose classifier can be adjusted to control the product size, the equations that are used to do this will require the feed and product 80% passing size of the circuit (Bond, 1962, Morrell, 2004[b], GMG Group,2016). In the case of open circuits suitable equations usually require the 80% passing size of the feed plus a variety of data relating to the geometry of the machine and its operating settings (Sinto et al 2015, Lane et al 2013, Morrell, 2004[a]).

ii. By multiplying this net specific energy and the target throughput the required net power draw is estimated. This is often called the "design" net power draw and it is the best estimate of what the average net power draw will be when the mill is in normal use. It is usual to inflate this figure to provide a contingency which accounts for potential operational fluctuations, catch-up capacity, uncertainty and/or variability in the ore hardness data, the accuracy of the power-based equations and the risk profile of the owners of the ore deposit in question. A factor that can complicate the choice of contingency concerns the ore hardness value chosen as the basis for design. Rather than use the mean hardness value from a series of tests on representative ore samples, some engineers use, say, an 85th percentile value or a 75th percentile value etc. This value is higher than the mean and inherently provides some degree of contingency. How much of a contingency this provides is uncertain as it will depend on the spread of the of the ore hardness distribution. From a statistical viewpoint this approach is unsatisfactory, though despite this it has become quite popular. In such cases additional contingencies may be applied and will vary from project to project. If a 75th- 85th percentile hardness value is used, then an additional contingency of the order of 5-15% may be applied. If the mean hardness is used the contingency may be up to 25%. Whatever value is used it is best decided on in collaboration with the deposit owners.
Once the contingency has been applied the resultant figure is the maximum net power that the machine will be required to deliver. The "net" for grinding mills most often relates to the power at the pinion gear shaft (or at the shell for gearless drives) and for HPGRs is usually at the roll shafts. As the purpose of this step is to determine the motor size required, further adjustments need to be made to the net power figure to allow for transmission/gearbox energy losses (usually in the range 3-7%). The resultant figure relates to the motor output power and is the required installed power.

iii. Equations (or manufacturers look-up tables) which relate the power draw to the dimensions of the machine and its operating conditions are then used to select a machine that in operation will be able to draw the required power. In choosing a suitable machine it is normal to ensure that the installed power is drawn when the equipment is operating at the extreme end of its operating envelope eg if a ball mill has been structurally designed to be operated with a maximum ball load of 40% then it should be able to draw the installed power with such a ball load. As the "design" power draw is lower than the installed power then in operation the mill will normally have a ball load lower than the maximum eg it might be 28-30%.

iv. In parallel with choosing a machine that will draw the required power it must also be ensured that the target throughput can be physically processed by the machine. This is a material transport problem and in the case of grinding mills it is usually sufficient to assume that if the machine can draw the required power it can also process the required throughput. However, some care needs to be exercised in using this assumption with closed circuit grate discharge mills, as flows may reach levels that require special attention to pulp lifter size and design (Latchireddi and Morrell, 2003). For HPGRs and conventional crushers the power draw/throughput assumption used for grinding mills is not appropriate. Hence further equations (or look-up tables) need to be applied to check that the selected machine is suitable from a throughput perspective. As with power draw, it is usual to also apply a similar contingency to the design throughput, the resultant throughput being the maximum that the machine can achieve. For example, in the case of an HPGR the maximum throughput might be matched to the machine operating at its maximum speed, the design throughput being achieved at a lower speed.

6.2 Power-Based Sizing and Selection of HPGRs

The general power-based methodology described in the previous section requires the application of 6 key equations for HPGR circuits. The derivation of these equations is described in detail in the following sections and applies solely to HPGRs fitted with studded/textured rolls and in closed circuit with classifiers. The resultant equations do not include any effects (should they exist) due to such design characteristics as cheek plates and roll flanges nor do they include the influence of classification efficiency. This later factor is known to affect circuit energy efficiency (Morrell, 2008) and in applying the equations described in this paper the designer must assume that the classification circuit will operate in a reasonably efficient manner.

In summary the equations relate to the following HPGR aspects:

- The relationship between roll diameter, roll length, roll speed and machine throughput capacity.

- The relationship between the specific grinding force and <u>machine</u> specific energy.
- The prediction of the <u>circuit</u> specific energy required to reduce the circuit feed F80 to the target circuit P80.
- The determination of the installed motor power.
- The estimation of the expected recycle load and the consequent throughput requirement of the machine.

6.2.1 Machine Throughput Capacity

Using a continuity equation and considering the passage of material as it passes between the operating gap of the HPGR, the throughput capacity can be described as follows (Klymowski, 2003):

$$Throughput\ \left(\frac{t}{h}\right) = 3.6 \times L \times s \times u \times \rho_c \tag{3}$$

Where:

L	=	Roll length (m)
s	=	Mean operating gap (mm)
u	=	Roll speed (m/s)
ρ_c	=	Cake specific gravity

Taking each term in equation 3 in turn, the roll length (L) is chosen from HPGR manufacturers' equipment catalogues. The mean operating gap (s) is normally reported as being a linear function of roll diameter, Klymowski (2003) assuming that it was a linear relationship. However, combining published data from a number of pilot and full-scale operations (Parker et al, 2001; Zervas, 2019; Kock et al, 2015; Englehardt et al, 2015; Hart et al, 2011) suggests that the following power function better describes the relationship (see Figure 4):

$$s = 32 \times D^{1.2} \tag{4}$$

where:

s	=	Mean operating gap for studded/textured rolls (mm)
D	=	Roll diameter (m)

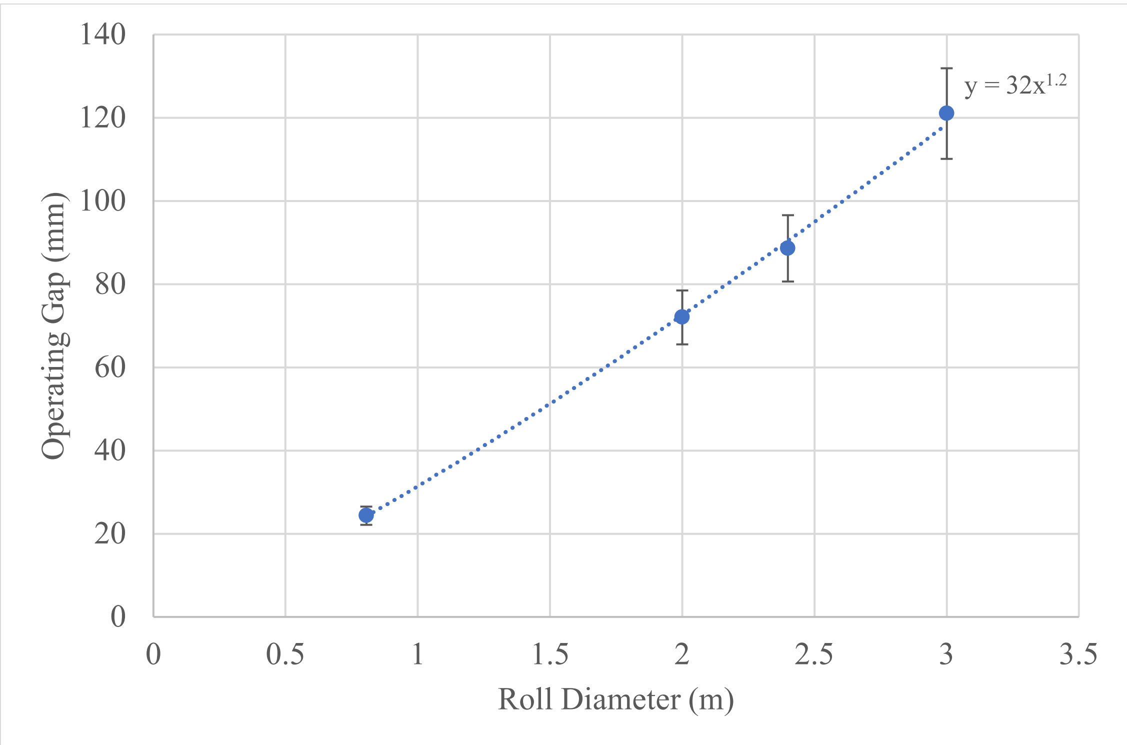

Figure 4 – Observed vs Predicted Operating Gap

It should be noted that the operating gap is principally related to the roll diameter but it is also a significant function of rolls surface. For example, a smooth roll can have up to a 40% smaller gap (all else being equal) than a studded/textured roll (equation 4 specifically relates to studded/textured roll surfaces). Secondary factors that can also affect the operating gap are feed size, feed size distribution, feed moisture, roll speed and operating pressure (Morley, 2010; Saramak and Kleiv, 2013).

HPGRs are often supplied with variable speed drives and two manufacturers quote the recommended speed range for each of their models in their equipment catalogues. Their nominal quoted maximum recommended speed appears to be a simple function of roll diameter; for example Figure 5 was compiled from data published by Metso (2021) and Polysius (2021). Their data suggest the relationship between the max roll speed (u_{max}) and diameter in the range 0.7-3.0m is:

$$u_{max}\ (m/s) = 0.68 \times D + 0.87 \tag{5}$$

Typically the minimum speed is of the order of 60% of u_{max}.

The cake (also known as flake) sg (r_c) is assumed to be 85% of the in-situ ore sg (r_o) (Otte, 1988; Klymowski et al, 2003; Daniel, 2007). Thus:

$$\rho_c \approx 0.85 \times \rho_o \tag{6}$$

Hence an ore with an in-situ sg of 2.7 would have a cake sg of approximately 2.3. If equations 4 and 6 are substituted into equation 3 we get:

$$\begin{aligned} Throughput\ (t/h) &= 3.6 \times L \times 32 \times D^{1.2} \times u \times 0.85 \times \rho_o \\ &= 98 \times L \times D^{1.2} \times u \times \rho_o \end{aligned} \tag{7}$$

By applying equation 5 to the published operating data from Morenci (Zervas,2019), Boddington (Hart et al, 2011), Tropicana (Ballantyne et al, 2017), Cerro Verde (Koski et al, 2011) and Cadia Hill (Engelhardt et al., 2015) the throughput prediction results shown in Figure 6 were obtained. The agreement is reasonably good, with a maximum error of 6%.

Combining equations 5 and 7 gives an equation which predicts the maximum throughput for a given roll diameter, roll length and ore sg as follows:

$$Maximum\ throughput\ (t/h) = 98 \times L \times D^{1.2} \times (0.68 \times D + 0.87) \times \rho_o \tag{8}$$

This equation is useful in estimating what the ultimate throughput capacity is of a machine that is being considered for a particular duty.

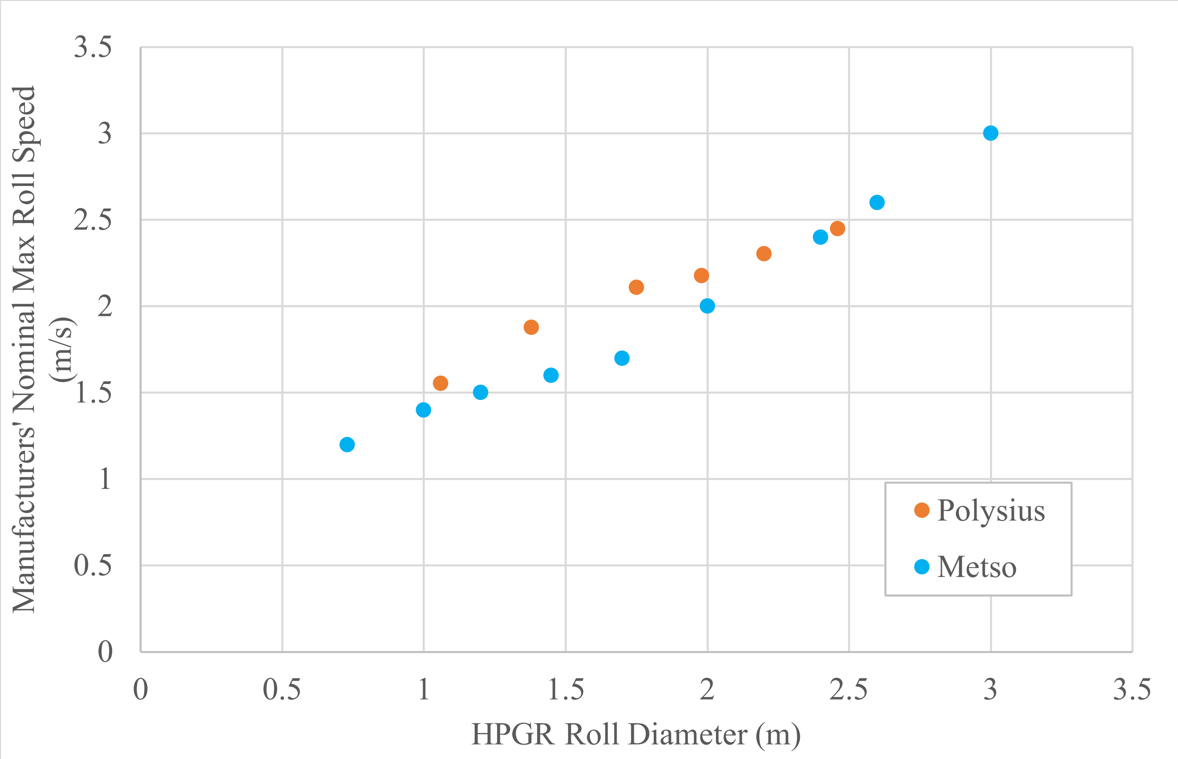

Figure 5 – Relationship Between Roll Diameter and Maximum Roll Speed as Indicated by Published Data from Polysius (2021) and Metso (2021) Equipment Catalogues

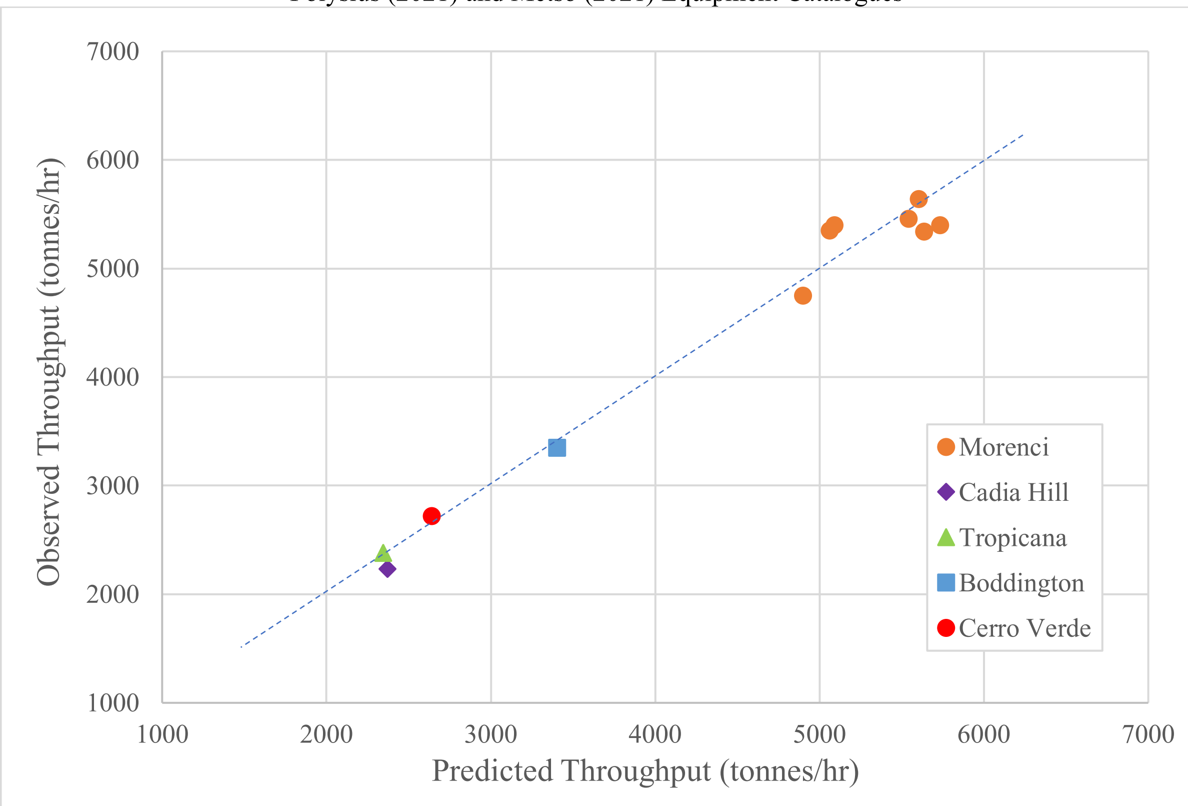

Figure 6 – Observed vs Predicted HPGR Machine Throughput

6.2.2 Specific Grinding Force

An HPGR principally comprises two horizontally mounted counter-rotating rolls, one being fixed, the other being free to move against a pressure applied by hydraulic pistons. Usually there are two pistons mounted on each side of the moving roll giving a total of four pistons. The pressure applied via the hydraulics can be varied which in turn varies the force applied to the feed ore via the rolls. This applied force is often quoted in terms of the specific grinding force which is defined as follows:

$$SF\ (N/mm^2) = \frac{F}{(1000 \times D \times L)} \tag{9}$$

Where

SF	=	Specific grinding force (N/mm^2)
F	=	Applied force (kN)
D	=	Roll diameter (m)
L	=	Roll length (m)

Sometimes manufacturers quote the pressure (usually in bars) applied by the hydraulic pistons rather than the applied force or specific grinding force. In such cases the specific grinding force can be determined as follows:

$$SF\ (N/mm^2) = \frac{(4 \times \pi \times (D_p/2)^2 \times 0.1 \times H)}{(D \times L)} \tag{10}$$

Where

D_p	=	Hydraulic piston diameter (m)
H	=	Hydraulic pressure (bar)

Note that equation 8 is based on there being 4 hydraulic pistons in total. Most full-scale machines are designed to operate up to a specific grinding force of 4 - 5 N/mm^2, the maximum varying slightly from manufacturer to manufacturer. Published data indicate that most full-scale machines in the minerals industry operate in the 2-4 N/mm^2 range (Hart et al, 2012; Kock et al, 2015; Burns et al, 2019; Mular et al, 2015; van der Meer and Maphosa, 2013).

It has been found that the specific grinding force of the HPGR is closely related to its net specific energy (Patzelt et al, 2000). Based on the published data from a number of full-scale installations (see Figure 7) this relationship can be described using a simple linear function as follows:

$$\mathrm{W}_{hm}\ (\mathrm{kWh}/t) = 0.37 \times SF \tag{11}$$

Where:

W_{hm}	=	Machine net specific energy ie machine net power draw/machine throughput
SF	=	Specific grinding force (N/mm^2)

The observed correlation is reasonably good, the scatter being due to secondary effects such as feed size, feed size distribution, moisture content and roll surface condition/design. The above relationship is the result of a unique feature of HPGRs in that the applied specific energy can be adjusted on line, independent of the throughput, giving them a degree of operational flexibility not found in grinding mills.

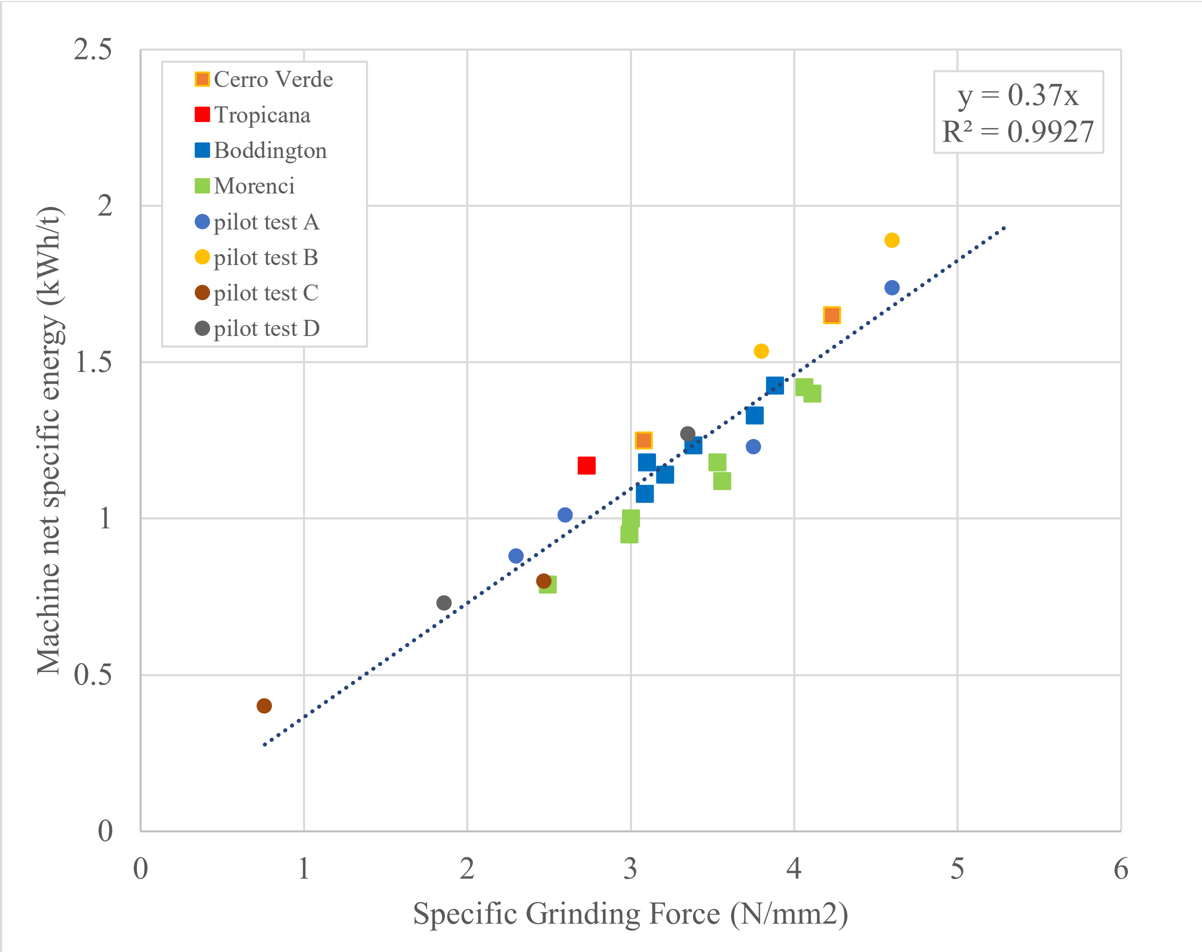

Figure 7 – Relationship Between Specific Grinding Force and Machine Specific Energy

6.2.3 Installed Motor Power

When the HPGR is operating at maximum speed it will be running at maximum throughput capacity. If at the same time it is being operated at maximum specific grinding force it will be delivering maximum machine net specific energy. Multiplying these two maxima together will give the maximum power that the machine will be potentially able to deliver. When designing an HPGR the manufacturer therefore needs to ensure that the installed motors are large enough to provide this maximum power.

The maximum throughput capacity is described by equation 8, whilst the maximum net specific energy is predicted from equation 11 by using the maximum specific grinding force (SF_{max}) that the machine has been designed to deliver:

$$Maximum\ machine\ net\ specific\ energy(kWh/t) = 0.37 \times SF_{max} \tag{12}$$

Combining equations 8 and 12, the maximum net power that the machine is capable of providing is given by:

$$Maximum\ net\ power\ (kW) = 36.3 \times L \times D^{1.2} \times SF_{max} \times (0.68 \times D + 0.87) \times \rho_o \tag{13}$$

The motor also has to provide power to overcome drive train losses, which has been assumed to be 7% of motor output power. Therefore by applying a factor of (100/(100-7) = 1.075 to equation 11 to account for this gives:

$$Installed\ power\ (kW) = 39 \times L \times D^{1.2} \times SF_{max} \times (0.68 \times D + 0.87) \times \rho_0 \tag{14}$$

Published data on equipment specifications from HPGR manufacturers CITIC (2021), KHD (2012), Koeppern (2021), Metso (2021) and Polysius (2021) were compiled to test the above relationship. Using an in-situ ore sg (r_o) of 2.8, equation 12 was used to predict the installed power and the results compared to the manufacturers’ recommended motor sizes. Figure 8 shows the outcome, indicating a close correlation. What is significant in this correlation apart from the fact that it appears to work quite well is that it suggests that all of the HPGR manufacturers broadly agree on the relationship between design, operating conditions and resultant power draw.

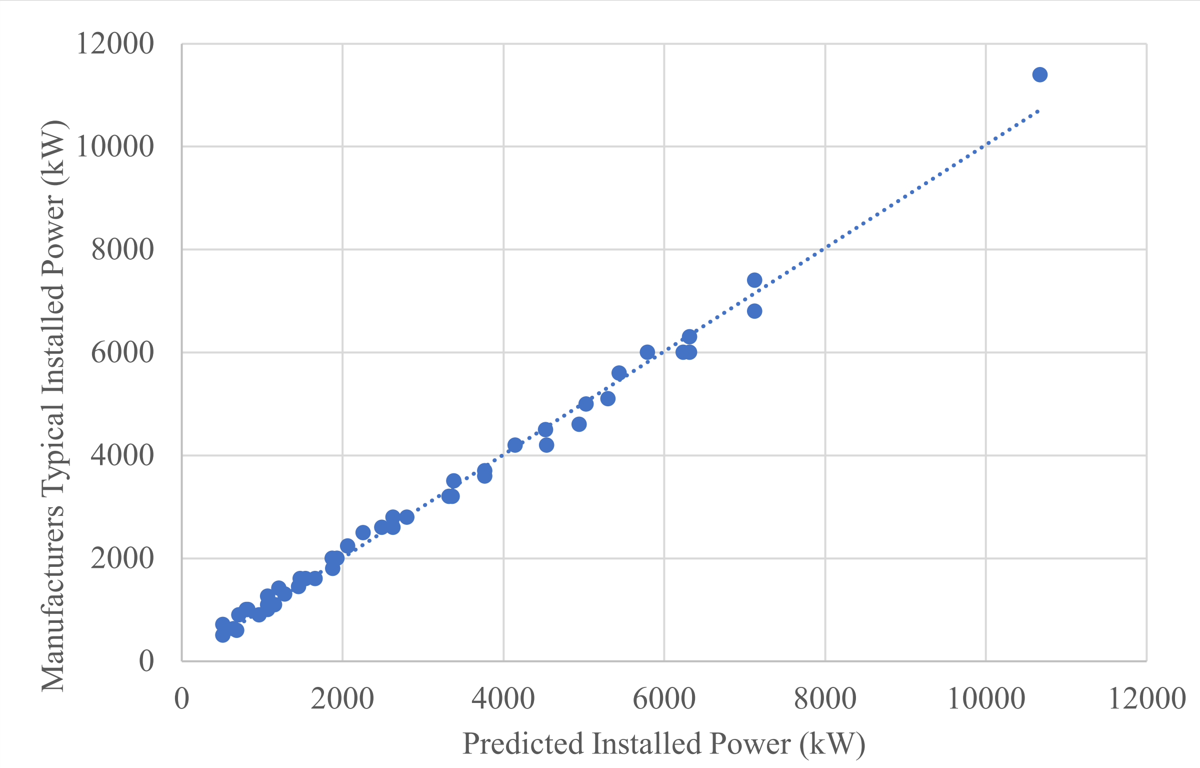

Figure 8 – Manufacturers Published Installed Power vs Predicted Using Equation 12

6.2.4 HPGR Circuit Specific Energy Requirement

In this paper only HPGR machines in closed circuit with classifiers are considered. The specific energy of such circuits is the HPGR machine power draw divided by the circuit fresh feedrate and is the specific energy required to reduce in size the fresh feed (F_{80}) to the classifier (fine) product (P_{80}). This specific energy can be estimated using Morrell's energy-size relationship (Morrell, 2004[b]; GMG Group, 2021). The general form of this is given in equation 2.

As applied to HPGR circuits equation 2 is formulated as follows:

$$W_{hc} = M_{ih} \times S_h \times k_3 \times k_4 \times 4 \times \left({P_{80}}^{f(P80)} - {F_{80}}^{f(F80)} \right) \quad (15)$$

Where:

W_{hc} = predicted net specific energy of the HPGR circuit (kWh/t)
M_{ih} = SMC Test® HPGR hardness parameter (kWh/t)
S_h = coarse feed factor
= $35 \times (F_{80} \times P_{80})^{-0.2}$: $(0.5 < S_h < 1)$
K_3 = open/closed circuit factor
= 1.19 for open circuit
= 1.0 for closed circuit
k_4 = $\dfrac{(0.71 \times e^{(0.28 \times SF)})}{({M_{ih}}^{0.23})}$
SF = the applied specific grinding force in the range 1.8–5.3 N/mm^2

It should be noted that the effect of K_4 is to predict a decrease in the required specific energy to achieve a certain size reduction as the applied specific force is decreased ie it predicts greater energy efficiency at lower specific forces. This is in line with reports by both Klymowski (2003), who noted that "*It is frequently more energy* *efficient to operate a HPGR at lower pressures….*" and Zervas (2019) in his analysis of the Morenci HPGR circuit data who concluded that "*Energy efficiency proved to decrease at greater specific forces*".

6.2.4.1 Validation

Figure 9 shows how well equation 15 predicts the specific energy of a range of HPGR circuits, including Morenci (Zervas,2019) and Tropicana (Ballantyne,2017). It gives a relative error standard deviation < 4%.

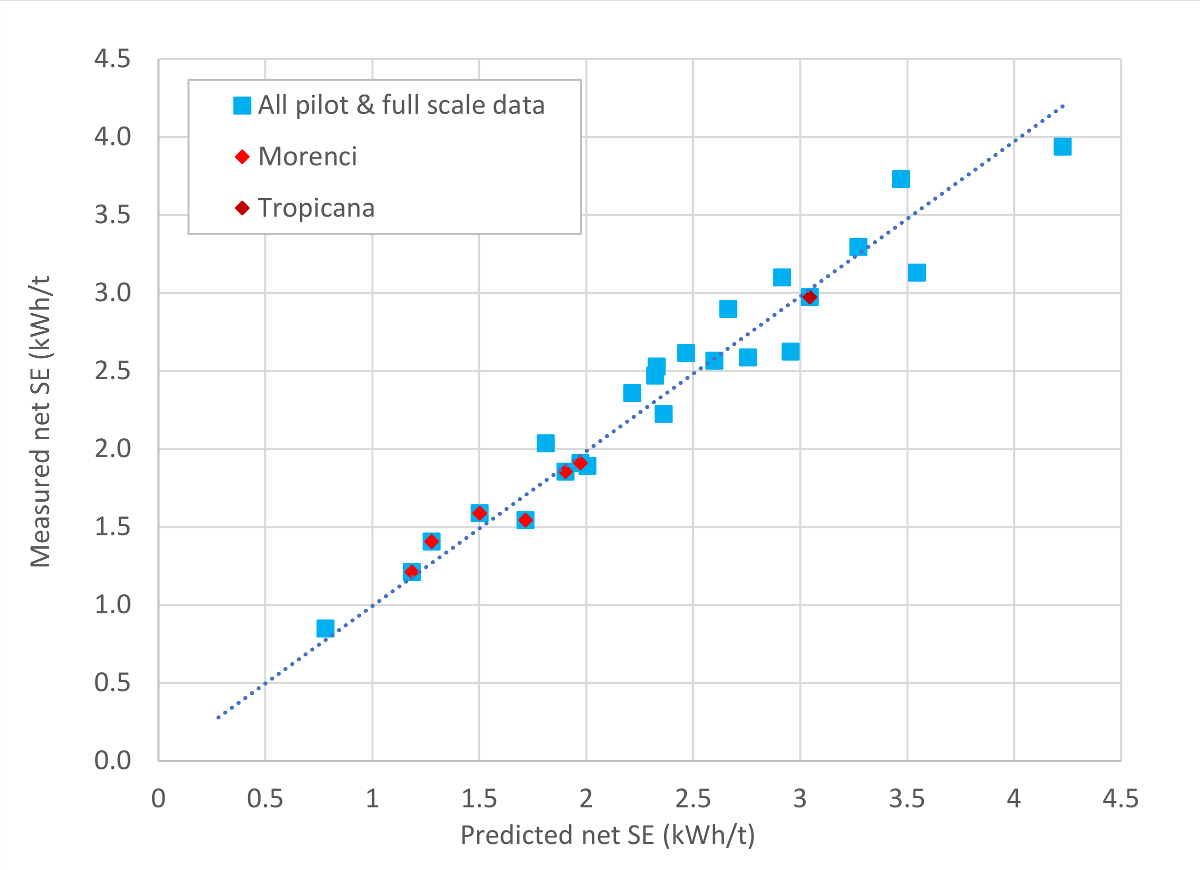

Figure 9 – Observed vs Predicted HPGR Circuit Net Specific Energy

Obviously if improved size reduction energy efficiency is obtained when an HPGR is operated at a lower specific grinding force then the converse is also true. Does this mean that more and more energy is wasted as the specific grinding force is progressively increased? Stephenson (1997) clearly showed that in most cases as the applied specific grinding force increased, the Bond laboratory ball work index of the HPGR product decreased in line with the degree of microcracking that he observed under an electron microscope. Hence although the HPGR energy expenditure to achieve a given size reduction increases as the applied specific force increases, the additional energy may not be all wasted but instead might be used to save energy in the ball mill circuit by weakening the ball mill feed. However, it is not yet clear as the specific grinding force increases whether the overall comminution circuit specific energy increases, decreases or stays the same.

6.2.5 Recycle Load and Machine Throughput Requirement

Considering the HPGR circuit in the comminution flowsheet shown in Figure 10, the recycle load is defined as:

$$Recycle\ Load\ (\%) = \frac{Tph_8}{Tph_5} \times 100 \qquad (16)$$

Where:

Tph_5 = HPGR circuit fresh feedrate

Tph_8 = HPGR circuit classifier oversize (recycle) flowrate

If the HPGR machine net power draw is represented by P then the HPGR circuit net specific energy (W_{hc}) is given by:

$$W_{hc} = \frac{P}{Tph_5} \tag{17}$$

Rearranging gives:

$$Tph_5 = \frac{P}{W_{hc}} \tag{18}$$

The HPGR machine net specific energy (W_{hm}) is given by:

$$W_{hm} = \frac{P}{Tph_6} \tag{19}$$

Rearranging gives:

$$Tph_6 = \frac{P}{W_{hm}} \tag{20}$$

Also:

$$Tph_6 = Tph_8 + Tph_5 \tag{21}$$

Combining equations 18, 20 and 21 gives:

$$Tph_8 = \frac{P}{W_{hm}} - \frac{P}{W_{hc}} \tag{22}$$

Combining equations 16, 18 and 22 gives:

$$Recycle\ Load\ (\%) = \frac{\left(\frac{P}{W_{hm}} - \frac{P}{W_{hc}}\right)}{\frac{P}{W_{hc}}} \times 100$$

Hence:

$$Recycle\ Load\ (\%) = \left(\frac{W_{hc}}{W_{hm}} - 1\right) \times 100 \tag{23}$$

As W_{hc} can be determined from equation 15 and W_{hm} from equation 11, the recycle load can be predicted using equation 23. In a design situation the HPGR circuit fresh feedrate (Tph_5) will be specified. By knowing the recycle load it is then possible to determine what the throughput requirement of the HPGR machine will be (Tph_6). This needs to be known so that a suitably sized machine can be chosen that is able to process material at this rate. This can be expressed as follows:

$$Machine\ throughput\ requirement\ (t/h) = Circuitfresh\ feedrate \times \left(1 + \frac{recycle\ load}{100}\right) \tag{24}$$

As mentioned in section 6.1, in design situations it is usual to apply a contingency which will vary from project to project. The chosen contingency is applied to the machine throughput requirement from equation 24 which gives the maximum machine throughput requirement. Given a particular size of HPGR, equation 8 can be used to predict what the machine's maximum throughput capability is and this needs to be greater than or equal to the maximum machine throughput requirement.

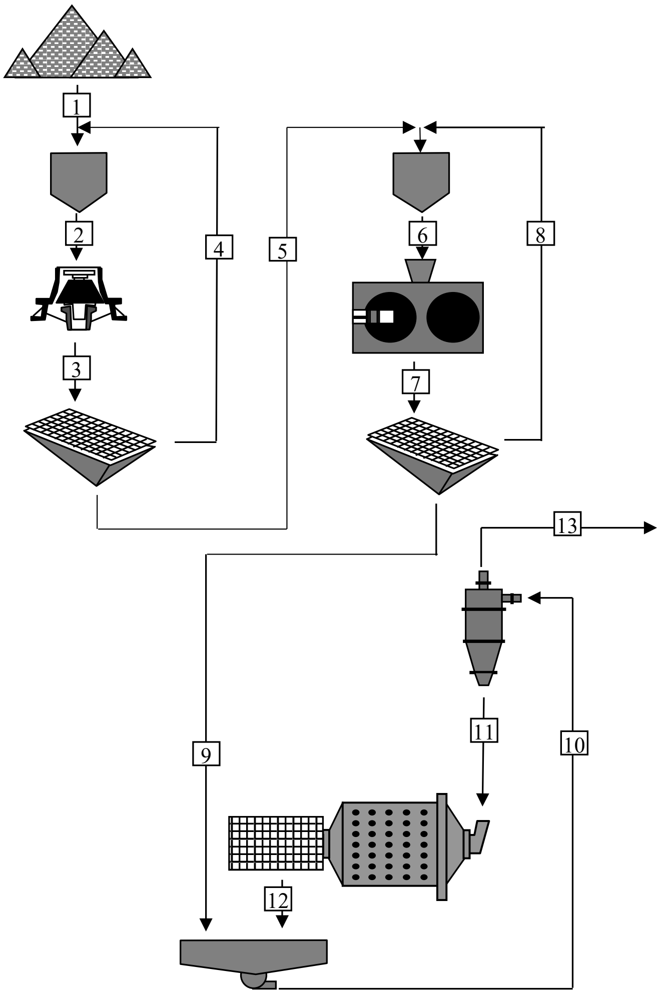

Figure 10 – Example of Crushing/HPGR/Ball Mill Circuit

6.3 Power-based Sizing and Selection of Ball Mill Circuits

The methodology for sizing and selecting ball mills is somewhat simpler than with HPGRs. This is because it is usual to assume that if the ball mill has been sized correctly to draw the required power it will automatically be able to transport the required throughput. Hence additional throughput equations are not normally required. Therefore for sizing a ball mill circuit there are only three steps:

1. Predict the circuit specific energy
2. Estimate the required installed power
3. Determine the ball mill dimensions, speed and maximum ball load that will result in drawing the installed power.

6.3.1 Ball Mill Circuit Specific Energy

The ball mill circuit specific energy requirement is predicted using equation 2. The calculation is done in two parts. The first part takes account of the specific energy to grind relatively coarse particles (>750 microns) and is represented by W_a whilst the second part takes account of grinding relatively fine particles (<750 microns) and is represented by W_b. The overall specific energy is the sum of the two. Hence to determine the specific energy to grind coarse particles (> 750 µm) in tumbling mills (W_a), equation 2 is written as:

$$W_a = M_{ia} \times 4 \times \left({P_{80}}^{f(P80)} - {F_{80}}^{f(F80)}\right) \qquad (25)$$

Where:

M_{ia} = SMC Test® coarse grinding hardness parameter

P80 = 750 microns

$f(P80) = -(0.295 + 750/1000000)$

F80 = 80% size of the ball mill feed (HPGR circuit product)
$f(F80) = -(0.295 + F80/1000000)$

For grinding finer particles (<750 microns) in tumbling mills (W_b) equation 2 is written as:

$$W_b = M_{ib} \times 4 \times \left(P_{80}{}^{f(P80)} - F_{80}{}^{f(F80)}\right) \quad (26)$$

Where:
M_{ib} = Hardness parameter derived using the raw data from a standard laboratory Bond ball mill work index test
P80 = ball mill cyclone overflow 80% passing size in microns (ball mill circuit product size)
$f(P80) = -(0.295 + P80/1000000)$
F80 = 750 microns
$f(F80) = -(0.295 + 750/1000000)$

The sum of W_a and W_b gives the overall ball mill specific energy to which an adjustment may then be applied to account for weakening of the ball mill feed by the action of the HPGR. Research on gold ores, iron ores, bauxite, quartz and marble has shown (Stephenson, 1997) that the amount of weakening is proportional to the magnitude of the HPGR pressing force (Figure 11). The Global Mining Guidelines Group advises that in absence of testwork on HPGR feed and product samples to determine the magnitude of this affect, an adjustment in the range 5-7% should be made (GMG Group, 2021). The relationship in Figure 11 can also be used.

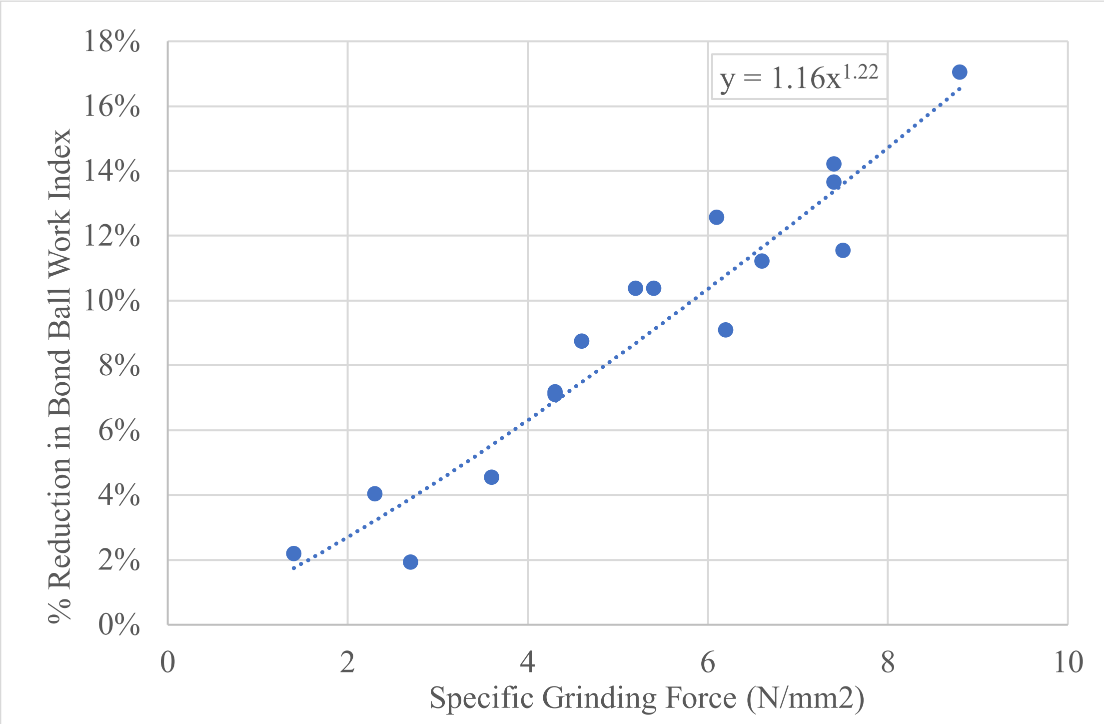

Figure 11 - Influence of HPGR Grinding Force on Bond Ball Mill Work Index Values (data after Stephenson, 1997)

Combining equations 25 and 26 and taking into account the weakening of ball mill feed by the HPGR, the overall ball mill specific energy is given by:

$$W_{bm} = K_{hpgr} \times (W_a + W_b) \quad (27)$$

Where
W_{bm} = Overall ball mill net specific energy (kWh/t)
K_{hpgr} = Factor to account for weakening of ball mill feed by the HPGR (typically in the range 0.93-0.95)
W_a = Net specific energy to grind from ball mill feed to 750 microns

W_b = Net specific energy to grind from 750 microns to ball mill circuit product

6.3.1.1 Determination of the M_{ib} Parameter

Whereas the M_{ih} parameter (equation 15) and M_{ia} parameter (equation 25) are obtained from a SMC Test®, the M_{ib} parameter is obtained from the raw data generated from a standard laboratory Bond ball mill work index (Wi_{BM}) test (Morrell, 2008) Hence:

$$M_{ib} = \frac{18.18}{P100^{0.295} \times Gpb \times \left(P80^{f(P80)} - F80^{f(F80)}\right)} \quad (28)$$

Where:

P100 = the closing screen aperture (μm)
Gpb = the net screen undersize product per revolution in the laboratory ball mill (g/rev)
P80 = 80% passing size of the closing screen undersize (μm)
F80 = 80% passing size of the fresh feed (μm)
$f(P80) = -(0.295 + P80/1000000)$
$f(F80) = -(0.295 + F80/1000000)$

Worked examples illustrating how this equation is used can be found in the free-access paper (Morrell, 2022).

6.3.1.2 Validation

Wong et al (2019) applied the so-called "Morrell method" as described by the GMG Group (2016) to Cerro Verde ball mill data and also compared it with Bond's and Rowland's methodologies. Unfortunately in the preparation of Wong et al's paper, calculation errors in determining the M_{ib} values were made. In addition the recommended adjustment to take account of ball mill feed weakening by the HPGR was not applied. Hence the predictions of the ball mill specific energy assigned to the Morrell method were incorrect as were the conclusions concerning the accuracy of this approach. This has been acknowledged by Wong and his co-authors (Wong et al, 2020). The results from the correct application of the Morrell method are given in Tables 3-5. The data relate to ball mills 1-4 in the Cerro Verde C1 circuit and ball mills 1 and 5 in the C2 circuit. In conducting these calculations a K_{hpgr} factor of 0.91 to account for weakening of ball mill feed by the HPGR was applied and was determined from data reported by Cerro Verde (Koski et al, 2011). Wong et al's calculations from applying Bond and Rowland's methodology are also given in Tables 3-5. As can be seen, on average the Morrell method results were 2.6% higher than the measured values. Bond's and Rowland's methodologies on average gave 17.8% and 9.6% higher results respectively.

Table 5– Cerro Verde Ore Characteristics (Data from Wong et al, 2019)

Parameter	Units	C1 BM1	C1 BM2	C1 BM3	C1 BM4	C2 BM1	C2 BM5
Bond Ball Work Index (Wi_{BM})	kWh/t	16.1	15.9	16.2	16.1	15.3	15.3
M_{ia}	kWh/t	16.8	16.8	16.8	16.8	16.8	16.8
M_{ib}	kWh/t	17.6	16.8	17.1	17.4	16.6	17.4

Table 6 –Cerro Verde Predicted and Measured Ball Mill Net Specific Energy (Data from Wong et al, 2019)

Source	Units	C1 BM1	C1 BM2	C1 BM3	C1 BM4	C2 BM1	C2 BM5	Average
Bond	kWh/t	9.3	8.7	8.6	9.1	9.2	10.1	9.2
Bond-Rowland	kWh/t	8.6	8.0	8.0	8.4	8.7	9.5	8.5
Morrell	kWh/t	8.0	7.5	7.4	7.8	8.2	9.0	8.0
Measured	kWh/t	7.0	7.0	7.3	7.2	9.3	8.9	7.8

Table 7 – Cerro Verde Percentage Difference Between Predicted and Measured Ball Mill Net Specific Energy (Data from Wong et al, 2019)

Source	Units	C1 BM1	C1 BM2	C1 BM3	C1 BM4	C2 BM1	C2 BM5	Average
Bond	%	33.9	24.9	18.2	26.2	-1.0	12.8	17.8
Bond-Rowland	%	23.4	15.1	9.0	16.3	-6.4	6.5	9.6
Morrell	%	14.3	7.1	1.4	8.3	-11.8	1.1	2.6

Further ball mill circuit data were also sourced from Ballantyne et al (2017) from work they did on the HPGR/Ball mill circuit at Tropicana as well as Kock et al (2015). Their results are presented in Table 6 together with predictions using Morrell's approach. A K_{hpgr} factor of 0.96 was applied to account for weakening of ball mill feed by the HPGR. This was based on the relationship in Figure 13 and the typical Tropicana HPGR operating specific grinding force of 2.7 N/mm^2 that was reported by Kock et al (2015). On average the predictions were 0.2% higher than the measured values. The data in Table 6 are interesting in that the measured values suggest that even though the grind size in survey 2 was finer than survey 1, less energy was used ie in survey 2 it appeared that the circuit was more energy efficient. Ballantyne et al suggested that this was due to the fact that the ball mill circuit in survey 2 was more energy efficient. In survey 2 the ball mill speed was reduced from 83% of critical to 76% and it was hypothesized that this might have resulted in a trajectory change which created more favourable breakage conditions. Whether this was the case remains to be seen as Ballantyne et al also hypothesized that as the ball mill had a Slip Energy Recovery (SER) motor it could also be possible that the apparent change in grinding efficient was in fact caused by changes in the SER efficiency with speed.

Table 8 – Tropicana Predicted and Measured Ball Mill Net Specific Energy (Data from Kock et al, 20195 and Ballantyne et al, 2017)

		Kock et al	Ballantyne et al		Average
Parameter	Units	Plant summary	Survey 1	Survey 2	
F80	microns	2190[1]	2190[1]	2190[1]	2190
P80	microns	73	103[1]	91[1]	89
Bond lab work index	kWh/t	16.94[2]	19.2	19.2	18.43
Morrell Mib	kWh/t	24.4	25.7	26.6	25.57
Measured[3]	kWh/t	17.02	15.15	13.37	15.18
Morrell predicted	kWh/t	15.95	14.16	15.52	15.21
Difference	%	-6.29	-6.53	16.08	0.20

Notes: [1] Interpolated from graphical plots of feed and product size distributions
[2] Weighted average of primary and transition/oxide ores
[3] Reported data assumed to be based on motor input power; 6.5% motor/drivetrain losses were applied to convert to net power

6.3.2 Installed Motor Power

Having estimated the required ball mill circuit net specific energy, it is then required to estimate the installed power. The initial step is to multiply the required ball mill circuit net specific energy by the target throughput. The resultant power draw is the best estimate of what the average net power draw will be when the ball mill circuit is running under normal, steady state operating conditions. It is usual to apply a contingency that accounts for potential operational fluctuations, catch-up capacity, uncertainty and/or variability in the ore hardness data and the risk profile of the owners of the ore deposit in question. Its magnitude therefore varies from project to project. As mentioned in section 4.1 it also depends on the hardness value on which the design is to be based eg a mean value or a 75th percentile, 85th percentile etc. If the mean hardness is selected on which to base the design then a typical contingency is about 25%. At this point the resultant power draw will be in net terms. For grinding mills this usually relates to the power at the pinion gear shaft for a gear-and-pinion drive or at the shell for a gearless (wrap-around) drive. As the purpose of this step is to determine the motor size required, where motor size relates to its output power capacity, adjustments have to be made to the net power figure to allow for transmission/gearbox energy losses (usually of the order of 3-4%). The resultant figure will then relate to the motor output power capacity – usually referred to as the installed power.

6.3.3 Ball Mill Dimensions and Operating Conditions

The final step is to choose a ball mill diameter, length and speed that will draw the installed power when loaded with the mill's maximum allowable ball load. The maximum ball load needs to be chosen in conjunction with the equipment supplier as it is related to the structural integrity of the mill shell, which in turn is related to such factors as the shell thickness, steel composition, design and dimensions. To predict power draw based on mill dimensions etc. a power model such as Morrell's "C" model (Morrell, 1996) is used. The equations of this model can be easily entered into a spreadsheet or alternatively can be accesses on-line via the link https://www.smctesting.com/tools/gross-power.
This model predicts the motor input (gross) power of ball mills with a high degree of accuracy (Morrell, 2003). As motor size is based on motor output power the gross power needs to be adjusted to account for motor energy losses (usually of the order of 3%).

7. PREDICTED ENERGY SAVINGS

The previous sections have described the equations and procedures to size HPGR-based comminution circuits. To test their ability to reflect trends seen in practice they were used to compare a conventional SABC circuit with a HPGR/ball and a HPGR/HPGR circuit. The chosen ore characteristics are those shown in Table 9. The objective of the circuits is to reduce in size a ROM with a P80 of 450mm to a final P80 of 150 microns. For the HPGR-based circuits detailed worked examples using the ore characteristics in Table 9 can be found in an open-access paper (Morrell, 2022). For the SABC circuit similar worked examples can be found in an open-access publication (GMG,2019) or can be determined using SMC Testing's on-line tool. (https://www.smctesting.com/tools/comminution-specific-energy)

Table 9 – Ore hardness Characteristics

Parameter	Units	Value
sg		2.8
DWi®	kWh/m3	6.8
Mia®	kWh/t	19.4
Mic®	kWh/t	7.2
Mih®	kWh/t	13.9
Mib®	kWh/t	18.5

The results from applying the equations are summarised in Table 10. It should be noted that these figures represent only the energies consumed by the machines and do not include ancillaries. As can be seen The predicted energy saving of the HPGR/Ball mill circuit when compared to the SABC circuit amounts to 22%. This is similar to that reported by a number of existing HPGR/Ball mill circuits overall (Parker et al, 2001, Koski et al, 2011, Kock et al, 2015). The HPGR/HPGR circuit is predicted to save even more energy – 38% compared to the SABC circuit. This is in line with that reported at Iron Bridge (Fortesque, 2019).

Table 10 – Predictions of Specific Energies for various Circuit Designs

Machine	kWh/t		
	SABC	HPGR/Ball	HPGR/HPGR
Crushing	0.42	0.64	0.64
Primary HPGR	-	3.17	3.17
Secondary HPGR	-	-	6.31
SAG milling	16.03	-	-
Ball milling	-	9.03	-
Total	16.45	12.84	10.12
% saving over SABC	0	22	38

9. CONCLUSIONS

HPGR-Ball mill circuits have the potential to reduce the Hard Rock Mining Industry's CO_2 emissions by 15.5 megatonnes/year when compared to AG/SAG/Ball mill circuits. This saving climbs to 32.8 megatonnes/year if HPGRs are also used instead of ball mills. Despite this huge potential saving, uptake of HPGR technology has been relatively slow. This may be due in part to the fact that costly and time consuming pilot testing is still the norm for assessing, selecting and sizing HPGR-Ball mill circuits. This is in contrast to AG/SAG/Ball mill circuits which are normally assessed, selected and sized using the relatively cheap and effective power-based methodology.

Equations have been derived which, on the basis of published data from manufacturers and full-scale operating plants, accurately reproduce HPGR throughput capacity, installed power and specific energy for a wide range of HPGRs in the hard rock mining sector. This includes the largest machines currently in operation.

Analysis of published data on the influence the specific grinding force has confirmed assertions by a number of engineers and researchers that higher specific grinding forces result in a drop in comminution efficiency. Hence, the HPGR has to use additional energy to achieve a similar size reduction than when operating at lower specific grinding forces. As further published research has indicated that higher specific grinding forces result in weakening of the HPGR products, the additional energy may not be necessarily wasted but may save some energy in the downstream ball mill circuit. How this affects the overall energy consumption comminution circuits is not clear at this stage.

In recognition of the influence of specific grinding force on HPGR efficiency, an additional term has been added to the so-called "Morrell method" for predicting HPGR circuit specific energy. This extends the applicable range of this method to 1.8-5.3 N/mm^2. This has been adopted by the Global Mining Guidelines Group.

Using a new equation that accounts for the influence of specific grinding force on HPGR energy efficiency the "Morrell method" is shown to predict closed circuit HPGR performance to within 6.5% on average.

Analysis of published data on the performance of ball mills that follow HPGR circuits indicates that the "Morrell method" predicts ball mill circuit performance to within 3% on average. This analysis includes allowances for weakening of the HPGR product due to microcracking of ore particles and hence suggests that this phenomenon is observed in full-scale operating comminution circuits.

The results of this work suggest that power-based techniques, embodied in the "Morrell method", are able to accurately predict HPGR/ball mill circuit performance and hence are a reliable approach for assessing, sizing and selecting suitable HPGRs and ball mills in green field design scenarios.

8. REFERENCES

Andersen, J. S. 1988., Development of a Cone Crusher Model, M.Eng.Sc thesis, JKMRC, University of Queensland, Australia

Aydoğan, N.A., Ergün, L and Benzer, H., 2006. High pressure grinding rolls (HPGR) applications in the cement industry. Minerals Engineering, Volume 19, pp 130-139

Ballantyne, G.R., Di Trento, M., Lovatt, I. and Putland, B., 2017. Recent Improvements in the Milling Circuit at Tropicana Mine. Proc. Metplant 2017, Perth, Australia

Banini, G.A., 2002. An integrated description of rock breakage in comminution machines**.** Ph.D thesis, JKMRC, University of Queensland, Australia

Bond, F. C., 1959. Confirmation of the Third Theory, AIME Annual Meeting, San Francisco, California, USA

Bond, F.C., 1961[a]. Crushing and Grinding Calculations Part 1. Brit. Chem Eng., 6 (6), 378-385

Bond, F.C., 1961[b]. Crushing and Grinding Calculations Part 2. Brit. Chem Eng., 6 (6), 543-548

Buckingham, L., Dupont, J-F., Steiger, J., Blain, B. and Brits, C., 2011. Improving Energy Efficiency in Barrick Grinding Circuits. Proc. SAG 2011, Vancouver, Canada.

Burns, N., Gauld, C., Alvim, M. D. and Tagami, M., 2019. Technical Report – Salobo III Expansion**.** https://s21.q4cdn.com/266470217/files/doc_downloads/2020/03/Salobo-Technical-Report-FINAL.pdf

CIM Magazine, 2018, https://magazine.cim.org/en/technology/on-a-roll-en-1/

CITIC. 2021. https://www.citic-hic.com/data/upload/2015-11/20151110072914949494.pdf

Comi, T. and Burchardt, E., 2015. A Premier for Chile: The HPGR Based Copper Concentrator of Sierra Gorda SCM. Proc. SAG 2015, Vancouver, Canada.

Daniel, M. J., 2007. Energy efficient mineral liberation using HPGR technology, PhD thesis, JKMRC, School of Engineering, University of Queensland, Australia

Daniel, M., Lane, G. and McLean, E., 2010. Efficiency, economics, energy and emissions-emerging criteria for comminution circuit decision making Proc. XXV IMPC. Brisbane, Queensland, Australia

Demus, T., Echterhof, T., Pfeifer, H. and Quicker, P., 2012. Investigatings on the Use of Biogenic Residues as Substitutes for Fossil Coal in the EAF Steelmaking Process. Proc. 10th European Electric Steelmaking Conference, Graz, Austria.

Dindorf, R. and Wos, P., 2020. Energy-Saving Hot Open Die Forging Process of Heavy Steel Forgings on an Industrial Hydraulic Forging Press. Energies, 13(7):17

Dowling, E.C., Korpi, P.A., McIvor, R.E. and Rose, D.J.,2001. Application of High Pressure grinding Rolls in an Autogenous-Pebble Milling Circuit. Proc. SAG 2001, Vancouver, Canada.

EIA, 2020. How much carbon dioxide is produced per kilowatt hour of U.S. electricity generation? https://www.eia.gov/tools/faqs/faq.php?id=74&t=11
Engelhardt, D., Seppelt, J., Waters, T., Apfelt, A., Lane, G., Yahyaei, M., and Powell, M., 2015. The Cadia HPGR-SAG Circuit – From Design to Operation – The Commissioning Challenge. Proc. SAG 2015, Vancouver, Canada.
Fortescue, 2019. Iron Bridge Project Approval. https://www.fmgl.com.au/docs/default-source/announcements/iron-bridge-project-approval.pdf?sfvrsn=8cdff6a3_4
Giblett, A. and Seidel, J., 2011. Measuring, Predicting and Managing Grinding Media Wear. Proc. SAG 2011, Vancouver, Canada
GMG Group. 2021. Morrell Method for Determining Comminution Circuit Specific Energy and Assessing Energy Utilization Efficiency of Existing Circuits https://gmggroup.org/guidelines-and-publications/morrell-method-to-determine-the-efficiency-of-industrial-grinding-circuits/
Griffith, A. A. 1921. The Phenomena of Rupture and Flow in Solids. Philosophical Transaction of the Royal Society, London. Series AI Vol. 221.
Hart S., Parker B., Rees T., Manesh A., & Mcgaffin I. 2011. Commissioning and Ramp Up of the HPGR Circuit at Newmont Boddington Gold, Proc. SAG 2011, Vancouver, Canada.
KHD. 2012. https://www.khd.com/tl_files/downloads/products/grinding-technology/grinding/roller-presses-cement/KHD_ROLLER_PRESS_April_2012.pdf
Koeppern. 2021. https://www.koeppern-international.com/fileadmin/_migrated/content_uploads/Koeppern_High-Pressure_Grinding_01.pdf
Koski, S., J Vanderbeek, J.L. and Enriquez, J. 2011. Cerro Verde Concentrator – Four Years Operating HPGRs. Proc. SAG 2011, Vancouver, Canada
Klymowsky, R. 2003. High Pressure Grinding Rolls for Minerals. https://www.ausimm.com/globalassets/insights-and-resources/minerals-processing-toolbox/polysiushpgr.pdf
Kock, F., Siddall, L., Lovatt, I., Giddy, M. and Di Trento, M. 2015. Rapid Ramp-Up of the Tropicana Circuit. Proc. SAG 2015, Vancouver, Canada.
Lane, G., Foggiatto, B., and Bueno, M. 2013. Power-based comminution calculations using Ausgrind. Proc Procemin 2013, Santiago, Chile
Latchireddi, S. and Morrell, S. 2003. Slurry flow in mills: grate-pulp lifter discharge systems (Part 2). Minerals Engineering, Volume 16, Issue 7, July, pp 635-642
Macivor, R.E.E., Dowling, E.C., Korpi, P.A., and Rose, D.J. 2001. Application of high pressure grinding rolls in an autogenous-pebble milling circuit. Proceedings SAG 2001. Vancouver, Canada.
Metso. 2021. https://www.mogroup.com/portfolio/hrc-series/hrce/
Mining Technology, 2021.Iron Bridge Magnetite Project. https://www.mining-technology.com/projects/iron-bridge-magnetite-project/
Morley, C., 2010. HPGR – FAQs. SAIMM, vol 110, pp 107-115
Morrell, S. 1996. Power draw of wet tumbling mills and its relationship to charge dynamics—Part 1: A continuum approach to mathematical modelling of mill power draw. Trans. Inst. Min. Metall. Section C 105:C43–C53.
Morrell, S. 2003. Grinding mills: how to accurately predict their power draw. Proceedings XXII International Mineral Processing Congress, Cape Town, South Africa, SAIMM, pp 50-59.
Morrell, S. 2004[a]. Predicting the specific energy of autogenous and semi-autogenous mills from small diameter drill core samples. Miner. Eng. 17(3):447–451.
Morrell, S. 2004[b]. An alternative energy-size relationship to that proposed by bond for the design and optimisation of grinding circuits. Int. J. Miner. Process. 74:133–141.
Morrell, S. 2008. A method for predicting the specific energy requirement of comminution circuits and assessing their energy utilisation efficiency. *Minerals Engineering,* 21(3), 224–233. http://dx.doi.org/10.1016/j.mineng.2007.10.001
Morrell, S. 2009. Predicting the overall specific energy requirement of crushing, high pressure grinding roll and tumbling mill circuits. Miner. Eng. 22(6):544–549.
Morrell, S. 2011. The Appropriateness of the Transfer Size in AG and SAG Mill Circuit Design. Proc. SAG 2011, Vancouver, Canada.
Morrell, S. 2022. Helping to reduce mining industry carbon emissions: A step-by-step guide to sizing and selection of energy efficient high pressure grinding rolls circuits. *Minerals Engineering,* 179) https://doi.org/10.1016/j.mineng.2022.107431
Mular, M.A., Hoffert, J.R, and Koski, S. M., 2015. Design and Operation of the Metcalf Concentrator. Proc. SAG 2015, Vancouver, Canada.
National Research Council 1981. *Comminution and Energy Consumption*. Washington, DC: The National Academies Press. https://doi.org/10.17226/19669

Otte, O. 1988. Polycom High Pressure Grinding Principles and Industrial Application, in: Third Mill Operators' Conference, Cobar, NSW, Australia, pp. 131–135
Palmer, E., Dixon, S. and Meadows, D., 2011. An Update of the SAG Milling Operation at the Penasquito Mine Located in the Zactecas State, Mexico. Proc. SAG 2011, Vancouver, Canada.
Parker, B., Rowe, P., Lane, G. and Morrell, S., 2001. The decision to opt for high pressure grinding rolls for the Boddington expansion. SAG 2001, Vancouver, Canada, pp 93-106
Patzelt, N., Knecht, J., Burchardt, E. and Klymowsky, R. 2000. Challenges for High Pressure Grinding in the New Millennium. Seventh Mill Operators Conference. Kalgoorlie, WA, Australia, pp. 47-55
Pehl, P., Arvesen, A., Humpenoder, F., Popp, A., Hertwich, E.G. and Luderer, G.,2017. Understanding future emissions from low-carbon power systems by integration of life cycle assessment and integrated energy modelling, Nature Energy, volume 2, pp. 939–945
Polysius. 2021.
https://ucpcdn.thyssenkrupp.com/_legacy/UCPthyssenkruppBAIS/assets.files/products___services/mineral_processing/griding_plants/polycom_en.pdf
Rashidi, S., Rajamani, R. K. and Fuerstenau, D.W., 2017 A Review of the Modelling of High Pressure Grinding Rolls. KONA Powder and Particle Journal, Volume 34, pp 125-140.
Rule, C.M., Fouchee, R.J. and Swart, W.C.E., 2015. HPGR Operation at Mogalakwena Concentrators. Proc. SAG 2015, Vancouver, Canada
Saramak, D. and Kleiv, R.A., 2013.The effect of feed moisture on the comminution efficiency of HPGR circuits. Minerals Engineering, vol 43-44, pp 105-111
Stephenson, I., 1997. The downstream effects of high pressure grinding rolls processing. PhD Thesis. JKMRC, University of Queensland, Australia.
Scinto, P., Festa, A., and Putland, B. 2015. OMC Power-based comminution calculations for design, modelling and circuit optimization. Proc. 47th Annual Meeting CMP. Ottawa, Canada
Tavares, L.M., King, R.P., 1998. Single-particle fracture under impact loading. Int. J. Miner. Process. 54 pp1–28
Tozlu, F.J. and Fresko, M., 2015. Autogenous and Semi-Autogenous Mills 2015 Update. Proc SAG 2015, Vancouver, Canada.
Van Der Meer F.P., 1997. HPGR Grinding of Pellet Feed. Experiences of KHD in the Iron Ore Industry. AusIMM Conference on Iron Ore Resources and Reserves Estimation. 25-26 September 1997, Perth, WA, Australia
Van der Meer, F.P., 2015. Pellet Feed Grinding by HPGR. Minerals Engineering, Volume 73, pp 21-30
Van der Meer, F.P. and Maphosa, W. 2012. High pressure grinding moving ahead in copper, iron, and gold processing. SAIMM, vol 112, pp 637-647.
Vanderbeek J.L., Linde T.B., Brack W.S., & Marsden J.O. 2006. HPGR Implementation at Cerro Verde, Proc. SAG 2006, Vancouver, Canada
Villanueva, A., Banini, G., Hollow, J., Butar-Butar, R. and Mosher, J., 2011. Effects of HPGR Introduction on Grinding Performance at PT Freeport Indonesia's Concentrator. Proc. SAG 2011. Vancouver, Canada.
Weir. 2021. https://www.global.weir/assets/files/product%20brochures/enduron-high-pressure-grinding-rolls-hpgr-product-brochure.pdf
Wong, H., Mackert, T., Lipiec, T., Remmers, J., Burchardt, E., Vanderbeek, J.L. 2019. Optimising Ball Mill Selection for a HPGR Ball Mill Circuit. Proc. SAG 2019, Vancouver, Canada
Wong, H. 2020. Private communication, 22nd September 2020.
World Energy Data, 2021, World Electricity Generation 2020 https://www.worldenergydata.org/world-electricity-generation/
World Steel Association. 2017. Steel's Contribution to a Low Carbon Future.
https://www.steel.org.au/resources/elibrary/resource-items/steel-s-contribution-to-a-low-carbon-future-and-cl/download-pdf.pdf/#:~:text=The%20greenhouse%20gas%20of%20most,of%20total%20world%20CO2%20emissions.
Zervas, G . 2019.The Metcalf Concentrator HRC™3000: Performance at Variable Specific Force. Proc. SAG 2019, Vancouver, Canada